Analysis and Design of Quad-Band Four-Section Transmission Line Impedance Transformer

Hussam Jwaied, Firas Muwanes, and Nihad Dib

Electrical Eng. Dept., Jordan Univ. of Science and Technology,
P. O. Box 3030, Irbid 22110, Jordan, E-mail: nihad@just.edu.jo

Abstract **–** The design of four-section transmission line matching transformer, operating at four arbitrary frequencies, is presented. Standard transmission line theory is used to obtain a closed form expression that is solved using particle swarm optimization technique to find the required transformer parameters (lengths, and characteristic impedances). Different examples are presented which validate the design approach. To further validate the analysis and design approach, a microstrip line four-section quad-band transmission line transformer is designed, analyzed, fabricated and measured.

I. INTRODUCTION

With the advent of multi-band operation in wireless communication systems, it becomes essential to have matching transformers that operate at several frequencies. Recently, several papers have been published in which different techniques were proposed to design dual-frequency matching transformers [1-4]. In [1], a λ/4 - shorted stub was added to a conventional single-shunt-stub matching network that enabled impedance matching at two separate frequencies simultaneously. In [2], a novel dual-band two-section transmission line transformer (TLT) was proposed and simple design equations for the impedances and lengths of the two sections were derived in [3]. In [4], an extension of this dual-band TLT to match complex impedances was presented and applied to wideband high-frequency amplifiers. Very recently, a triple-band three-section TLT, extended from the two-section TLT concept, was designed and analyzed in [5]. Using simple transmission line theory, design expressions for the three-section TLT for three arbitrary operating frequencies were derived. Two non-linear equations were solved simultaneously via an optimization process to obtain the parameters of the transformer. As an application of these TLTs, dual-band two-section TLT and triple-band three-section TLT have been successfully used to design dual-band and triple-band Wilkinson power dividers, respectively, [6-8].

In this paper, the quad-band four-section TLT, which is matched at four arbitrary frequencies (f_1, f_2, f_3 and f_4) for any transforming ratio (Z_L/Z_0) is designed and analyzed. Four non-linear equations are derived using standard transmission line theory, which are then solved simultaneously using the particle swarm optimization (PSO) technique. The PSO technique is used to find the characteristic impedances and lengths of the first two sections, from which the impedances and lengths of the other sections are obtained using the antimetry conditions [9]. The PSO algorithm is a multiple-agents optimization algorithm that was introduced by Kennedy and Eberhart [10] in 1995 while studying the social behavior of groups of animals and insects such as flocks of birds, schools of fish, and swarms of bees. Recently, this technique found many successful applications in Electromagnetics [11-13]. PSO is similar in some ways to genetic algorithms, but requires less computational bookkeeping and generally fewer lines of code, including the fact that the basic algorithm is very easy to understand and implement. It should be mentioned that other optimization techniques could be used too, but recently, we have been interested in the application of PSO method in the design of different microwave passive elements [14, 15], and antennas [16]. The interested reader can refer to [10-16], and the references therein, for details of the PSO algorithm.

II. ANALYSIS AND DESIGN

Figure 1 shows a four-section transmission line transformer (TLT) that will be used to match a purely resistive load Z_L to a lossless transmission line with characteristic impedance Z_0. The characteristic impedances of the transmission-line sections are denoted as Z_1, Z_2, Z_3, and Z_4, with physical lengths l_1, l_2, l_3, and l_4, respectively. The problem is to find the lengths and impedances of the four sections such that a perfect match is obtained at four arbitrary frequencies f_1, f_2, f_3, and f_4.

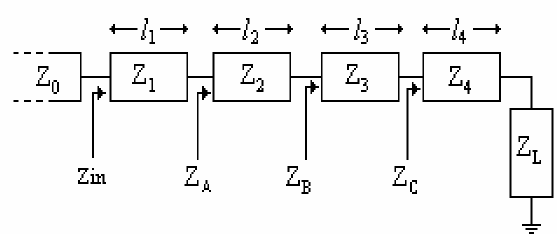

Fig. 1. Four-section quad-band TLT.

Using standard transmission line theory, the input impedance of the four-section TLT is given by,

$$Z_{in} = Z_1 \frac{Z_A + jZ_1 \tan(\beta\ell_1)}{Z_1 + jZ_A \tan(\beta\ell_1)} \tag{1}$$

where

$$Z_A = Z_2 \frac{Z_B + jZ_2 \tan(\beta\ell_2)}{Z_2 + jZ_B \tan(\beta\ell_2)}, \tag{2}$$

$$Z_B = Z_3 \frac{Z_C + jZ_3 \tan(\beta\ell_3)}{Z_3 + jZ_C \tan(\beta\ell_3)}, \tag{3}$$

$$Z_C = Z_4 \frac{Z_L + jZ_4 \tan(\beta\ell_4)}{Z_4 + jZ_L \tan(\beta\ell_4)}. \tag{4}$$

For perfect matching at specific frequencies, the lengths and impedances should be chosen such that $Z_{in} = Z_0$ at those frequencies. Imposing this condition on equation (1) and solving for Z_A gives,

$$Z_A = Z_1 \frac{Z_0 - jZ_1 \tan(\beta\ell_1)}{Z_1 - jZ_0 \tan(\beta\ell_1)}. \tag{5}$$

Solving equation (2) for Z_B gives,

$$Z_B = Z_2 \frac{Z_A - jZ_2 \tan(\beta\ell_2)}{Z_2 - jZ_A \tan(\beta\ell_2)}. \tag{6}$$

Substituting equation (5) in equation (6), gives,

$$Z_B = Z_2 \frac{Z_1 \dfrac{Z_0 - jZ_1 \tan(\beta\ell_1)}{Z_1 - jZ_0 \tan(\beta\ell_1)} - jZ_2 \tan(\beta\ell_2)}{Z_2 - jZ_1 \dfrac{Z_0 - jZ_1 \tan(\beta\ell_1)}{Z_1 - jZ_0 \tan(\beta\ell_1)} \tan(\beta\ell_2)}. \tag{7}$$

Another equation for Z_B can be obtained by substituting equation (4) in equation (3), which gives,

$$Z_B = Z_3 \frac{Z_4 \dfrac{Z_L + jZ_4 \tan(\beta\ell_4)}{Z_4 + jZ_L \tan(\beta\ell_4)} + jZ_3 \tan(\beta\ell_3)}{Z_3 + jZ_4 \dfrac{Z_L + jZ_4 \tan(\beta\ell_4)}{Z_4 + jZ_L \tan(\beta\ell_4)} \tan(\beta\ell_3)}. \tag{8}$$

Equating the complex equations (7) and (8), we get the following two expressions,

$$\begin{aligned}
&\left(\frac{Z_2}{Z_1} - \frac{Z_1}{Z_2}k\right)\tan(\beta\ell_1)\tan(\beta\ell_2) \\
&+\left(\frac{Z_3}{Z_1} - \frac{Z_1}{Z_3}k\right)\tan(\beta\ell_1)\tan(\beta\ell_3) \\
&+\left(\frac{Z_4}{Z_1} - \frac{Z_1}{Z_4}k\right)\tan(\beta\ell_1)\tan(\beta\ell_4) \\
&+\left(\frac{Z_3}{Z_2} - \frac{Z_2}{Z_3}k\right)\tan(\beta\ell_2)\tan(\beta\ell_3) \\
&+\left(\frac{Z_4}{Z_2} - \frac{Z_2}{Z_4}k\right)\tan(\beta\ell_2)\tan(\beta\ell_4) \\
&+\left(\frac{Z_4}{Z_3} - \frac{Z_3}{Z_4}k\right)\tan(\beta\ell_3)\tan(\beta\ell_4) \\
&+\left(\frac{Z_1Z_3}{Z_2Z_4}k - \frac{Z_2Z_4}{Z_1Z_3}\right)\times\begin{Bmatrix}\tan(\beta\ell_1)\tan(\beta\ell_2) \\ \times\tan(\beta\ell_3)\tan(\beta\ell_4)\end{Bmatrix} = (1-k),
\end{aligned} \tag{9}$$

$$\begin{aligned}
&\left(\frac{Z_L}{Z_1} - \frac{Z_1}{Z_0}\right)\tan(\beta\ell_1) + \left(\frac{Z_L}{Z_2} - \frac{Z_2}{Z_0}\right)\tan(\beta\ell_2) \\
&+\left(\frac{Z_L}{Z_3} - \frac{Z_3}{Z_0}\right)\tan(\beta\ell_3) + \left(\frac{Z_L}{Z_4} - \frac{Z_4}{Z_0}\right)\tan(\beta\ell_4) \\
&+\left(\frac{Z_1Z_3}{Z_0Z_2} - \frac{Z_2Z_L}{Z_1Z_3}\right)\tan(\beta\ell_1)\tan(\beta\ell_2)\tan(\beta\ell_3) \\
&+\left(\frac{Z_1Z_4}{Z_0Z_2} - \frac{Z_2Z_L}{Z_1Z_4}\right)\tan(\beta\ell_1)\tan(\beta\ell_2)\tan(\beta_4) \\
&+\left(\frac{Z_1Z_4}{Z_0Z_3} - \frac{Z_3Z_L}{Z_1Z_4}\right)\tan(\beta\ell_1)\tan(\beta\ell_3)\tan(\beta\ell_4) \\
&+\left(\frac{Z_2Z_4}{Z_0Z_3} - \frac{Z_3Z_L}{Z_2Z_4}\right)\tan(\beta\ell_1)\tan(\beta\ell_2)\tan(\beta\ell_3) = 0
\end{aligned} \tag{10}$$

where k is the impedance transforming ratio (or the normalized load impedance) defined as $k=Z_L/Z_0$.

For a compact size, the characteristics impedances must be monotonically increasing or monotonically decreasing, i.e., they should satisfy one of the following conditions [5],

For $k<1$: $Z_L < Z_4 < Z_3 < Z_2 < Z_1 < Z_0$
For $k>1$: $Z_0 < Z_1 < Z_2 < Z_3 < Z_4 < Z_L$

Moreover, since an optimized transformer, in the sense of achieving global minima of the reflection coefficient at the design frequencies, is being designed, it should satisfy the antimetry conditions given as, [9],

$$l_1 = l_4 \text{ and } l_2 = l_3\,, \tag{11a}$$

$$Z_1Z_4 = Z_2Z_3 = Z_0Z_L. \tag{11b}$$

It is worth mentioning that the dual-band TLT [3] and the tri-band TLT [5] were found to satisfy these conditions too. Enforcing the above antimetry conditions on the left side of equation (10) gives a zero; that is equation (10) is satisfied if the lengths and the impedances satisfy the antimetry conditions. This validates, to some extent, that indeed the antimetry conditions have to be satisfied. On the other hand, enforcing the antimetry conditions in equation (9), and after some simplification, the following expression is obtained,

$$\begin{aligned} &2a + b\frac{\tan(\beta\ell_1)}{\tan(\beta\ell_2)} + c\frac{\tan(\beta\ell_2)}{\tan(\beta\ell_1)} \\ &+ d\tan(\beta\ell_1)\tan(\beta\ell_2) + \frac{(k-1)}{\tan(\beta\ell_1)\tan(\beta\ell_2)} = 0 \end{aligned} \tag{12}$$

where

$$a = \left(\frac{z_2}{z_1} - \frac{z_1}{z_2}k\right) + \left(\frac{k}{z_1 z_2} - z_1 z_2\right), \tag{13a}$$

$$b = \frac{k}{z_1^2} - z_1^2\,, \tag{13b}$$

$$c = \frac{k}{z_2^2} - z_2^2\,, \tag{13c}$$

$$d = \frac{z_1^2}{z_2^2}k - \frac{z_2^2}{z_1^2}\,. \tag{13d}$$

In equation (13), normalized impedances are used where $z_1=Z_1/Z_0$, and $z_2=Z_2/Z_0$. It is clear that there are four unknowns in equation (12); namely: z_1, z_2, l_1, and l_2. Now, equation (12) should be satisfied at the four design frequencies f_1, f_2, f_3, and f_4 which can be written as follows: $f_2=u_1 f_1$, $f_3=u_2 f_1$, and $f_4=u_3 f_1$, where u_1, u_2, and u_3 are any positive real numbers.

At f_1, we get,

$$\begin{aligned} &2a + b\frac{\tan(\beta_1\ell_1)}{\tan(\beta_1\ell_2)} + c\frac{\tan(\beta_1\ell_2)}{\tan(\beta_1\ell_1)} \\ &+ d\tan(\beta_1\ell_1)\tan(\beta_1\ell_2) + \frac{(k-1)}{\tan(\beta_1\ell_1)\tan(\beta_1\ell_2)} = 0. \end{aligned} \tag{14}$$

At f_2, we get,

$$\begin{aligned} &2a + b\frac{\tan(u_1\beta_1\ell_1)}{\tan(u_1\beta_1\ell_2)} + c\frac{\tan(u_1\beta_1\ell_2)}{\tan(u_1\beta_1\ell_1)} \\ &+ d\tan(u_1\beta_1\ell_1)\tan(u_1\beta_1\ell_2) + \frac{(k-1)}{\tan(u_1\beta_1\ell_1)\tan(u_1\beta_1\ell_2)} = 0. \end{aligned} \tag{15}$$

At f_3, we get,

$$\begin{aligned} &2a + b\frac{\tan(u_2\beta_1\ell_1)}{\tan(u_2\beta_1\ell_2)} + c\frac{\tan(u_2\beta_1\ell_2)}{\tan(u_2\beta_1\ell_1)} \\ &+ d\tan(u_2\beta_1\ell_1)\tan(u_2\beta_1\ell_2) + \frac{(k-1)}{\tan(u_2\beta_1\ell_1)\tan(u_2\beta_1\ell_2)} = 0. \end{aligned} \tag{16}$$

At f_4, we get,

$$\begin{aligned} &2a + b\frac{\tan(u_3\beta_1\ell_1)}{\tan(u_3\beta_1\ell_2)} + c\frac{\tan(u_3\beta_1\ell_2)}{\tan(u_3\beta_1\ell_1)} \\ &+ d\tan(u_3\beta_1\ell_1)\tan(u_3\beta_1\ell_2) + \frac{(k-1)}{\tan(u_3\beta_1\ell_1)\tan(u_3\beta_1\ell_2)} = 0. \end{aligned} \tag{17}$$

Finally, given k, u_1, u_2 and u_3, the previous four non-linear equations (14) to (17), need to be solved simultaneously for the four unknowns z_1, z_2, l_1/λ_1 and l_2/λ_1 via an optimization process, where λ_1 is the wavelength at f_1.

As mentioned in the introduction, the particle swarm optimization (PSO) technique is used here to solve these four equations. The fitness function is chosen to be the sum of the absolute values of the left sides of equations (14) to (17). Once the four unknowns (z_1, z_2, l_1, and l_2) are obtained, the other four unknowns z_3, z_4, l_3, and l_4 can be calculated using the antimetry conditions. In all the results presented in the next section, 20 particles are used in the PSO code, and the search is stopped once the value of the fitness function becomes less than 10^{-10}. Depending on the initial swarm positions, 1500-2000 iterations were usually needed to reach an acceptable solution. Typically, this took around 15-30 seconds using Pentium-3 PC. The algorithm was run more than once to make sure that it converges to the same solution each time.

III. RESULTS

Using the approach described in the previous section, several designs have been performed to achieve matching at four arbitrary frequencies. Table 1 shows the obtained results for the case with $u_1 = 2$, $u_2 = 3$, and $u_3 = 4$, while the impedance ratio k is changed from 0.5 to 10. Figure 2 shows the return loss versus frequency for different values of k. It can be noticed that there is a perfect match at the four design frequencies. From the figure, as expected, one can observe that the response for k and its inverse $1/k$ are the same. Moreover, from the results in Table 1, we notice that changing the impedance ratio k changes the characteristic impedances, while the lengths of the sections are not affected.

Another case that has been considered is to fix u_2, u_3 and k, while changing u_1. Table 2 includes some results in which u_1 is changed between 1.4 and 2.6, with $u_2 = 3$, $u_3 = 4$, $k = 2$. It can be noticed that as u_1 increases, the impedance and length of the first section decrease, while the impedance and length of the second section increase. Figure 3 shows the frequency response for some of these cases.

Table 1. Impedances and normalized lengths of a quad-band four-section TLT with Z_0 = 50 Ω, u_1 = 2, u_2 = 3, and u_3 = 4.

k	Z_1	Z_2	Z_3	Z_4	l_1/λ_1	l_2/λ_1
0.5	43.47	37.87	33.01	28.76	0.1	0.1
2	57.51	66.02	75.74	86.94	0.1	0.1
4	66.68	87.51	114.27	149.95	0.1	0.1
6	73.22	103.54	144.86	204.87	0.1	0.1
8	78.56	116.89	171.09	254.56	0.1	0.1
10	83.21	128.58	194.42	300.44	0.1	0.1

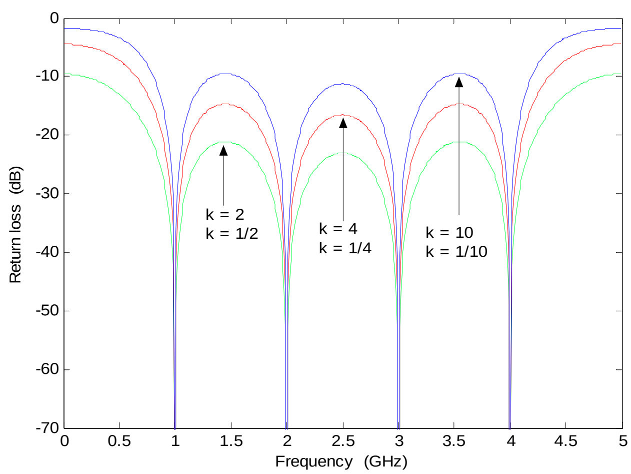

Fig. 2. Return loss of the four-section transformer presented in Table 1 with f_1=1 GHz.

Table 2. Impedances and normalized lengths of a four-section TLT with u_2 = 3, u_3 = 4, k = 2, Z_0 = 50 Ω.

u_1	Z_1	Z_2	Z_3	Z_4
1.4	59.09	63.78	78.39	84.60
1.8	57.98	65.2	76.68	86.24
2.2	57.17	66.69	74.97	87.45
2.6	56.81	67.71	73.85	88.02

u_1	l_1/λ_1	l_2/λ_1
1.4	0.1493	0.0660
1.8	0.1079	0.0964
2.2	0.0943	0.1019
2.6	0.0858	0.1035

Similarly, one can fix u_1, u_3, and k, while changing u_2. Table 3 includes some results in which u_2 is changed between 2.4 and 3.6, with u_1 = 2, u_3 = 4, and k = 2. In this case, as u_2 increases, Z_1 and l_2 increase, while Z_2 and l_1 decrease. Figure 4 shows the frequency response for some of these cases.

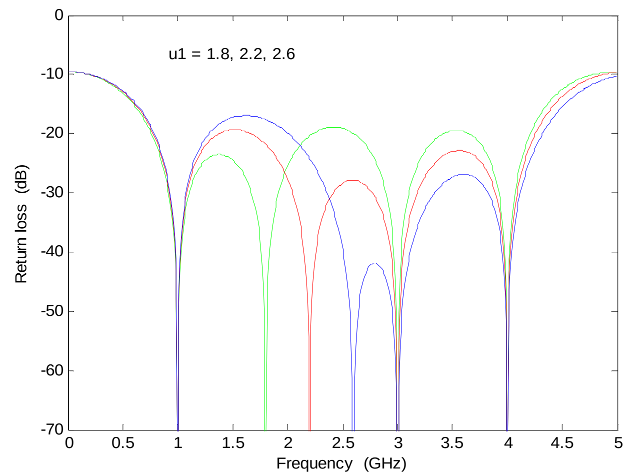

Fig. 3. Return loss of the four-section transformer presented in Table 2 with f_1=1 GHz.

Table 3. Impedances and normalized lengths of a four-section TLT with u_1 = 2, u_3 = 4, k = 2, Z_0 = 50 Ω.

u_2	Z_1	Z_2	Z_3	Z_4
2.4	56.77	67.84	73.70	88.07
2.8	57.25	66.55	75.13	87.33
3.2	57.78	65.56	76.53	86.53
3.6	58.36	64.81	77.14	85.67

u_2	l_1/λ_1	l_2/λ_1
2.4	0.1221	0.0921
2.8	0.1068	0.0974
3.2	0.0937	0.1025
3.6	0.0822	0.1074

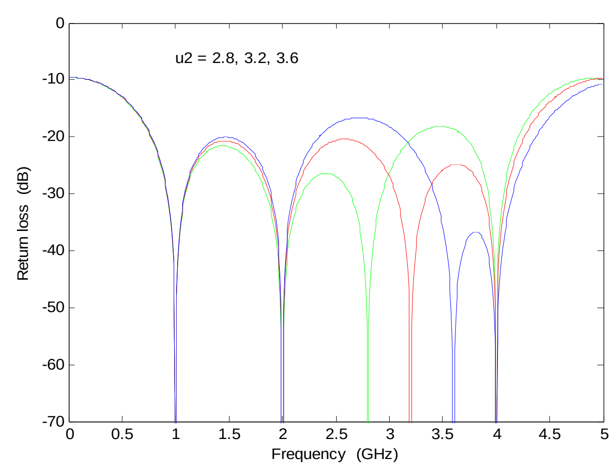

Fig. 4. Return loss of the four-section transformer presented in Table 3 with f_1=1 GHz.

Finally, k, u_1 and u_2 are fixed, and u_3 is changed to different arbitrary values. Table 4 shows some cases in which u_3 is changed between 3.4 and 4.6, with $u_1 = 2$, $u_2 = 3$, and $k = 2$. Figure 5 shows the frequency response for these cases.

Table 4. Impedances and normalized lengths of a four-section TLT with $u_1 = 2$, $u_2 = 3$, $k = 2$, $Z_0 = 50\ \Omega$.

u_3	Z_1	Z_2	Z_3	Z_4
3.4	56.01	65.29	76.58	89.24
3.8	56.95	65.69	76.11	87.77
4.2	58.06	66.49	75.19	86.11
4.6	59.00	68.13	73.38	84.74

u_3	l_1/λ_1	l_2/λ_1
3.4	0.0987	0.1145
3.8	0.0982	0.1059
4.2	0.1033	0.0928
4.6	0.1140	0.0765

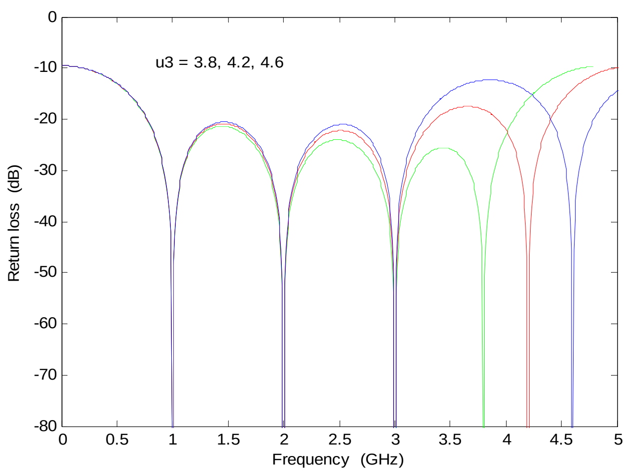

Fig. 5. Return loss of the four-section transformer presented in Table 4 with f_1=1 GHz.

To further validate our analysis, a quad-band four-section microstrip line transformer is designed, fabricated and measured. This transformer is designed to match a load impedance $Z_L = 100\ \Omega$ to a $50\ \Omega$ microstrip transmission line at $f_1 = 0.3$ GHz, $f_2 = 0.6$ GHz, $f_3 = 0.95$ GHz, and $f_4 = 1.25$ GHz. The ideal transmission line sections impedances and lengths are found to be as follows: $Z_1 = 56.8519\ \Omega$, $Z_2 = 66.8843\ \Omega$, $Z_3 = 74.7559\ \Omega$, $Z_4 = 87.9478\ \Omega$, $l_1 = l_4 = 69.677$ degrees, $l_2 = l_3 = 34.839$ degrees, where the electrical lengths refer to f_1.

Using the software *Ansoft Designer SV* [17], and assuming a 1.6 mm thick FR-4 substrate, the physical lengths and microstrip widths are found to be as follows: ℓ_1=107.225 mm, ℓ_2 = 54.2794 mm, ℓ_3 = 54.7366 mm, ℓ_4 = 110.761 mm. W_1 = 2.312 mm, W_2 = 1.697 mm, W_3 = 1.343 mm, and W_4 = 0.9157 mm. It should be noted that although the electrical lengths of opposite sections are equal, their physical lengths differ slightly due to the difference in the effective dielectric constant of each section, which depends on the microstrip line width. Figure 6 presents the simulation results obtained using *Designer SV*, which shows a very good match at the four design frequencies. Using the available PCB facility, this quad-band microstrip line TLT was fabricated, in which a surface mount resistor was used as the load. The overall size of the practical circuit seen in Fig. 7 is 25×7 cm. Figure 8 presents the measured return loss, which clearly shows the quad-band impedance matching. Some of the design frequencies are slightly shifted which could be due to losses of the connectors, and the inaccuracies in the widths and lengths of the microstrip line sections.

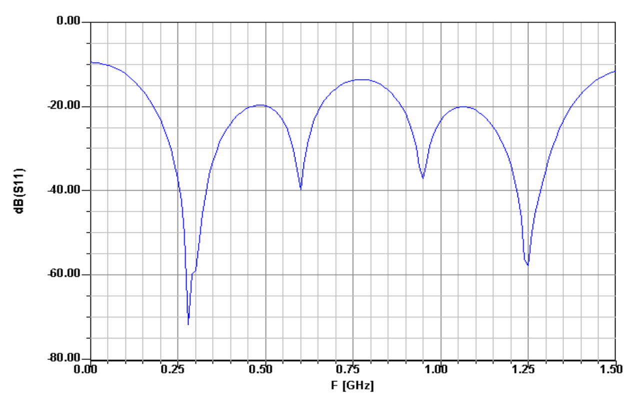

Fig. 6. Simulation results for a quad-band microstrip TLT with a 1.6 mm thick FR-4 substrate (ε_r = 4.6).

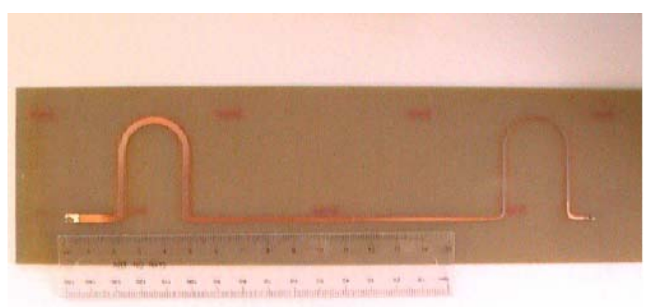

Fig. 7. Photograph of the fabricated quad-band microstrip line TLT. The first and last sections are bent to reduce the total length of the TLT.

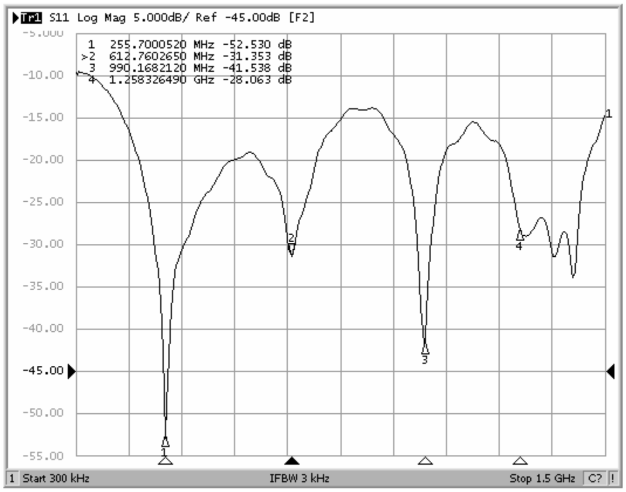

Fig. 8. Measured return loss for the fabricated quad-band microstrip line TLT.

IV. CONCLUSIONS

The contributions presented in this paper can be summarized as follows:

(a) A simple configuration for a quad-band transmission line transformer (TLT) has been proposed which uses four transmission line sections. Using ideal transmission line theory, a single equation, that needs to be satisfied simultaneously at the four design frequencies, has been derived. This equation involved only four unknowns (z_1, z_2, l_1/λ_1, and l_2/λ_1) to be solved for.

(b) The particle swarm optimization (PSO) technique, which is drawing much attention at the present time, has been used to design the quad-band TLT by searching for the four parameters z_1, z_2, l_1/λ_1 and l_2/λ_1. The other four variables z_3, z_4, l_3/λ_1, and l_4/λ_1 were obtained using the antimetry conditions. In effect, the obtained impedances and lengths minimize the reflection coefficient at the four design frequencies.

(c) Finally, to validate the analysis, several quad-band four-section TLTs have been designed. The results were as expected; perfect match at the four frequencies. It has been found that the lengths of the sections do not depend on the transforming ratio *k* for fixed design frequencies. Moreover, a microstrip line quad-band TLT has been designed, simulated using *Ansoft Designer SV*, fabricated and measured. At the present time, we are investigating the possibility of building a quad-band Wilkinson divider based on the quad-band TLT studied here. Moreover, the design a quad-band transformer that is able to match complex impedances, similar to that presented in [4], will be investigated.

REFERENCES

[1] H. Nakajima, and M. Muraguchi, "Dual-Frequency matching technique and its application to an octave-band (30-60 GHz) MMIC amplifier," *IEICE Trans. Electron.*, vol. E80-C, no. 12, pp. 1614-1621, Dec. 1997.

[2] Y. Chow, and K. Wan, "A transformer of one-third wavelength in two sections – for a frequency and its first harmonic," *IEEE Microwave and Wireless Components Letters*, vol. 12, no. 1, pp. 22-23, Jan. 2002.

[3] C. Monzon, "A small dual-frequency transformer in two sections," *IEEE Trans. on Microwave Theory and Techniques*, vol. 51, no. 4, pp. 1157-1161, April 2003.

[4] P. Colantonio, F. Giannini, and L. Scucchia, "Matching network design criteria for wideband high-frequency amplifiers," *Int. J. RF and Microwave CAE*, vol. 15, pp. 423-433, 2005.

[5] M. Chongcheawchamnan, S. Patisang, S. Srisathit, R. Phromloungsri, and S. Bunnjaweht, "Analysis and design of a three-section transmission-line transformer," *IEEE Trans. on Microwave Theory and Techniques*, vol. 53, no. 7, pp. 2458-2462, July 2005.

[6] S. Srisathit, S. Virunphun, K. Bandudej, M. Chongcheawchamnan, and A. Worapishet, "A dual-band 3-dB three-port power divider based on a two-section transmission line transformer," *2003 IEEE MTT-S Int. Microwave Symp. Digest*, pp. 35-38, 2003.

[7] L. Wu, Z. Sun, H. Yilmaz, and M. Berroth, "A dual-frequency wilkinson power divider," *IEEE Transactions on Microwave Theory and Techniques,* vol. 45, no. 1, pp. 278-284, Jan. 2006.

[8] M. Chongcheawchamnan, S. Partisang, M. Krairiksh, and I. Robertson, "Tri-band wilkinson power divider using a three-section transmission-line transformer," *IEEE Microwave and Wireless Components Letters,* vol. 16, no. 8, pp. 452-454, Aug. 2006.

[9] V. Meschanov, I. Rasukova, and V. Tupikin, "Stepped transformers on TEM-transmission lines," *IEEE Trans. Microw. Theory Tech.,* vol. 44, no. 6, pp. 793-798, June 1996.

[10] J. Kennedy and R. C. Eberhart, "Particle swarm optimization," in *Proc. IEEE Int. Conf. Neural Networks*, vol. IV, Perth, Australia, Nov./Dec. 1995, pp. 1942–1948.

[11] D. Gies and Y. Rahmat-Samii, "Particle swarm optimization for reconfigurable phase-differentiated array design," *Microwave Opt. Technol. Lett.*, vol. 38, pp. 168–175, Aug. 2003.

[12] J. Robinson and Y. Rahmat-Samii, "Particle swarm optimization in electromagnetics," *IEEE Trans. Antennas Propag.*, vol. 52, no. 2, pp. 397–407, Feb. 2004.

[13] M. Khodier and C. Christodoulou, “Linear array geometry synthesis with minimum sidelobe level and null control using particle swarm optimization,” *IEEE Trans. Antennas Propagat.*, vol. 53, no. 8, pp. 2674-2679, August 2005.

[14] J. Ababneh, M. Khodier, and N. Dib, “Synthesis of interdigital capacitors based on particle swarm optimization and artificial neural networks,” *International Journal of RF and Microwave Computer-Aided Engineering*, vol. 16, pp. 322-330, July 2006.

[15] N. Dib and J. Ababneh, “Physical modeling and particle swarm design of coplanar waveguide square spiral inductor,” accepted for publication in *Int. J. of Modeling and Simulation*, to appear beginning of 2008.

[16] Y. Najjar, M. Moneer, and N. Dib, “Design of optimum gain pyramidal horn with improved formulas using particle swarm optimization,” accepted for publication in *International Journal of RF and Microwave Computer-Aided Engineering*, to appear in July 2007 issue.

[17] Available at www.ansoft.com.

Hussam Jwaied was born in Ajloun, Jordan, on July 9, 1984. He received his B. Sc. degree in telecommunication and electronics engineering from Jordan University of Science and Technology, Irbid, Jordan, in 2007. His research interests include RF and microwave integrated circuits.

Firas Muwanes was born in Zarqa, Jordan on June 5, 1984. He received the B. Sc. degree in telecommunication and electronics engineering from Jordan University of Science and Technology, Irbid, Jordan, in 2007. His current research interests include RF and microwave integrated circuits.

Nihad Dib obtained his B. Sc. and M. Sc. in EE from Kuwait University in 1985 and 1987, respectively. He obtained his Ph. D. in EE (major in Electromagnetics and Microwaves) in 1992 from University of Michigan, Ann Arbor. Then, he worked as an assistant research scientist in the radiation laboratory at the same school. In Sep. 1995, he joined the EE department at Jordan University of Science and Technology (JUST) as an assistant professor, and became a full professor in Aug. 2006. In 2002-2003, he was a senior research engineer with Ansoft Corporation, USA. His research interests are in computational electromagnetics and modeling of passive microwave components and circuits.